RSC Advances

ROYAL SOCIETY OF CHEMISTRY

www.rsc.org/advances

Graphical Abstract

Raspberry-like gold nanoparticles (Au RLNPs) synthesized through reduction of $HAuCl_4$ by using Brij35 surfactant and NaOH show high catalytic activities in the reduction of 4-nitrophenol and ethanol electrooxidation. The enhanced catalytic activities of Au RLNPs are mainly due to their high surface roughness. To improve the stability and applicability in a wide range of environments without degrading the distinct raspberry-like morphology, silica-coated Au RLNPs (Au RLNP@SiO_2 NPs) were successfully synthesized through a sol-gel process using poly(vinylpyrrolidone) (PVP) as a primer. In comparison with Au RLNPs and other Au nanoparticles, Au RLNP@SiO_2 NPs are more easily recovered and recycled in repeated catalytic reactions.

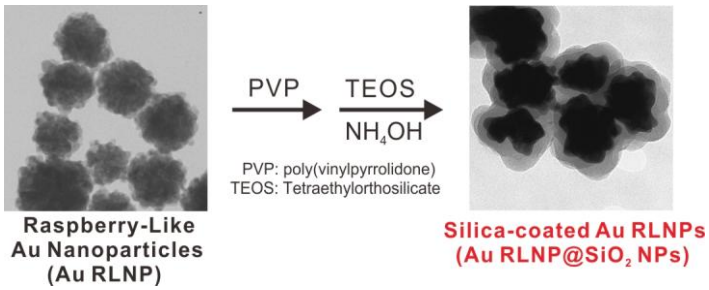

RSC Advances

RSCPublishing

ARTICLE

High Catalytic Performance of Raspberry-Like Gold Nanoparticles and Enhancement of Stability by Silica Coating

Hien Duy Mai, Kiouk Seo, Soon Choi, and Hyojong Yoo*

Cite this: DOI: 10.1039/x0xx00000x

Received 00th January 2012,
Accepted 00th January 2012

DOI: 10.1039/x0xx00000x

www.rsc.org/

Raspberry-like gold nanoparticles (Au RLNPs) synthesized through reduction of $HAuCl_4$ by using Brij35 surfactant and NaOH show high catalytic activities in the reduction of 4-nitrophenol and ethanol electrooxidation. The enhanced catalytic activities of Au RLNPs are mainly due to their high surface roughness. However, Au RLNPs are easily changed to spherical or aggregated nanoparticles by treatment with acids, thiols, and cationic surfactants (e.g., CTAB), making it difficult to sustain the catalytic activity. To improve the stability and applicability in a wide range of environments without degrading the original Au RLNP morphology, silica-coated Au RLNPs (Au RLNP@SiO_2 NPs) were successfully synthesized through a sol-gel process using poly(vinylpyrrolidone) (PVP) as a primer. In comparison with Au RLNPs and other Au nanoparticles, Au RLNP@SiO_2 NPs are more easily recovered and recycled in repeated catalytic reactions.

Introduction

Metallic nanoparticles have gained much attention over the past two decades due to their potential for a wide variety of applications including energy conversion,[1,2] chemical and biological sensing,[3,4] bioengineering,[5] and catalysis.[6,7] Extensive research efforts have been devoted towards the exploration of how to design metallic nanoparticles with diverse topographies,[8-10] and have yielded fascinating insights into their novel size- and shape-dependent properties.[11-13] Moreover, it has been theoretically and experimentally found that arrays of asymmetric geometries often impart a unique anisotropy to material properties.[13] It is also well recognized that the size, shape, composition, and crystallinity of nanoparticles strongly affect their catalytic performance.[14,15] This is due to surface anisotropies possessing a high density of low-coordinated atoms, with e.g., edges, boundaries, and defects serving as catalytically active sites that can markedly affect the chemical and physical properties of nanoparticles.[16]

Colloidal gold (Au) nanoparticles with varied morphologies are used in a diversity of heterogeneous green catalytic processes because of their excellent performance and high selectivity.[17-19] Engineering nanocatalytic systems with anisotropic geometries for specific applications is a critical task in nanotechnology. Recently, we successfully synthesized raspberry-like gold nanoparticles (Au RLNPs) through controllable reduction of $HAuCl_4$ by Brij35 surfactant under basic conditions.[20] The synthesized Au RLNPs possess high surface areas and show unique, highly red-shifted surface plasmon resonances (SPRs) due to their distinct raspberry-like structure with a plenitude of edges and tips. Au RLNPs are stable and retain their raspberry-like geometry in basic or neutral conditions; however, they gradually reshape to a spherical geometry under decreased pH. To maintain the surface roughness of Au RLNPs, further modifications such as introducing core-shell structural motifs are required.

Metallic nanomaterials are often encapsulated within silica shells, since silica-coated nanoparticles show substantial enhancement in their structural stability and suspension properties,[21] particularly in aqueous solvents. Moreover, silica-coated nanoparticles are readily modified through silane-coupling reactions to expand their surface functionalities.[22,23] Additionally, silica shells are chemically inert, biocompatible, and readily converted to a mesoporous layer offering external chemical species free access to the inner metal surfaces.[21,24] For direct encapsulation of Au nanoparticles within silica shells, conventional techniques employ coupling agents having a silane group (e.g. mercaptosilanes) for condensation of silica via the Stöber method.[25,26] However, we found experimentally that straightforward application of this method to Au RLNPs brought challenges, due to unusual aggregations of Au RLNPs. .

Herein, we report the synthesis of Au RLNP@SiO_2 NPs in solution through a simple solution-phase sol-gel process. To protect the high-energy surfaces of Au RLNPs, poly(vinylpyrrolidone) (PVP) was used as a polymeric stabilizer prior to the condensation of tetraethylorthosilicate (TEOS). Au RLNP@SiO_2 NPs showed a great enhancement of stability under strongly acidic conditions. The catalytic

performance, recovery, and reusability of both Au RLNP@SiO_2 NPs and Au RLNPs were investigated using the reduction reaction of 4-nitrophenol (4-NP) as a reaction model. We also found that Au RLNPs were capable of catalyzing ethanol electrooxidation in alkaline media.

Experimental Section

Reagents

Polyoxyethylene glycol dodecyl ether ($(C_2H_4O)_{23}C_{12}H_{25}OH$, Brij35, Acros Organics), hydrogen tetrachloroaurate trihydrate ($HAuCl_4 \cdot 3H_2O$, 99.9%, Sigma–Aldrich), poly(vinylpyrolidone) ($(C_6H_9NO)_n$, PVP10, average mol wt. 10,000, Sigma–Aldrich), 4-nitrophenol ($O_2NC_6H_4OH$, 99%, Sigma–Aldrich), sodium hydroxide (NaOH, 97%, Sigma–Aldrich), ammonium hydroxide (NH_4OH, 28-30 wt% ammonia, Sigma–Aldrich), tetraethylorthosilicate (Si(OC2H5)4 98%, Sigma–Aldrich), hexadecyltrimethylammonium bromide (CTAB, $(C_{16}H_{33})N(CH_3)_3Br$, 99%, Acros Organics), (3-mercaptopropyl)methyldimethoxysilane (MPTS, $CH_3Si(OCH_3)_2CH_2CH_2CH_2SH$, 95%, Alfa Aesar), HCl, HNO_3, and ethyl alcohol were used as received. All stock solutions were freshly prepared before each reaction. Prior to use, all glassware was washed with Aqua Regia (volume ratio of 3:1 of concentrated HCl and HNO_3; *Caution: Aqua Regia is highly toxic and corrosive and must be handled in fume hoods with proper personal protection equipment*) and rinsed thoroughly with deionized water.

Synthesis of raspberry-like gold nanoparticles (Au RLNPs)

Au RLNPs were prepared as described in our previous publication.[20] Briefly, an aqueous Brij35 solution (1 mL; 19.3 wt%) was well mixed with NaOH (aq) (100 μL; 100 mM) by shaking for 30 seconds. To this mixture, $HAuCl_4$ (aq) (50 μL; 10 mM) was added, and shaken vigorously for 1 minute. The pale yellow reaction mixture turned blue within 5 minutes at room temperature. To ensure a complete reaction, this mixture was allowed to react for over 20 minutes in total before the products were collected by centrifugation (5 min; 13500 rpm), and redispersed in nanopure water.

Treatment of Au RLNPs with CTAB, MPTS, and HCl

For CTAB-treated Au RLNPs, CTAB (*aq*) (10, 50, 100, and 200 mM; 100 μL) was introduced into the colloidal aqueous solutions of as-synthesized Au RLNPs (1 mL of nanopure water). For the reaction of Au RNLPs with MPTS (MPTS-treated Au RLNPs), as-synthesized Au RLNPs were dispersed in EtOH (1 mL) and MPTS (1, 5, 10, and 25 μL) was then added into the solution. The UV-Vis spectrum of each solution was observed at different reaction times over a period of 24 hours. For HCl-treated Au RLNPs, HCl (100 mM; 100 μL) was added into a colloidal solution of as-synthesized Au RLNPs (1 mL); the blue reaction mixture quickly turned to red. The mixtures were sampled at different reaction times and purified by centrifugation (5 min; 13500 rpm), redispersed three times in nanopure water, and imaged.

Synthesis of Au RLNP@SiO_2 NPs

The preparation of Au RLNP@SiO_2 NPs was as follows: first, the as-synthesized Au RLNPs were dispersed in 1 mL of deionized water. Next, 200 μL of 1.28 mM PVP aqueous solution was added to the Au RLNP solution. The resulting mixture was then stirred at room temperature for 12 hours to ensure complete adsorption of PVP on the Au RLNPs. Afterward, the PVP-capped Au RLNPs were purified by centrifugation (5 min; 13500 rpm), and redispersed in a solvent mixture consisting of 1 mL deionized water and 7 mL ethyl alcohol. In the next step, tetraethylorthosilicate (TEOS, 30 μL) and ammonium hydroxide (200 μL of 14.8 M NH_4OH (aq.)) were sequentially added to the aqueous solution of PVP-capped Au RLNPs. The reaction mixture was further stirred at room temperature for 4 h. After completion of the reaction, the resultant Au RLNP@SiO_2 NPs were centrifuged, and then purified by repeated washing in nanopure water. For HCl-treated Au RLNP@SiO_2 NPs, HCl (100 mM; 100 μL) was added into a colloidal solution of as-synthesized Au RLNP@SiO_2 NPs (1 mL) and incubated for 2 hours at room temperature. No color changes were observed.

Catalytic reduction of 4-nitrophenol

The catalytic reduction of 4-nitrophenol (4-NP) over nanoparticles in the presence of $NaBH_4$ was carried out to assess the catalytic activity of nanoparticles. In a typical experiment, 2 mL of deionized water, 1.7 mL of 0.2 mM 4-NP, and 1 mL of 15 mM $NaBH_4$ solution were mixed, followed by addition of the as-synthesized Au RLNPs dispersed in 1 mL of deionized water. The mixture was well swirled and transferred into a quartz cuvette. The color of the solution changed gradually from yellowish to clear as the reaction proceeded. UV-Vis spectra were recorded at 30-second intervals to monitor the progress of the reaction.

For comparison experiments, consistent amounts of Au RLNPs (evaluated by UV-Vis spectra) were used to obtain equivalent quantities of Au RLNP@SiO_2 NPs and HCl-treated Au RLNPs in the synthesis/treatment steps described above. The catalytic performances of Au RLNP@SiO_2 NPs and HCl-treated Au RLNPs were similarly evaluated.

Ethanol electrocatalytic oxidation

All electrochemical measurements were carried out in a conventional three-electrode cell at ambient temperature (~25˚C) using a WPG 100e Potentiostat (WonAtech Inc.). Au RLNPs-modified working electrode was fabricated as follows: Prior to electrochemical experiments, a glassy carbon (GC) electrode was sonicated in ethanol and deionized water in succession. Then, 10 μL of Au RLNP suspension was dropped onto the carbon disk and dried at room temperature. Platinum wire and a Ag/AgCl electrode were employed as counter and reference electrodes, respectively. With an aqueous mixture of 0.5 M KOH and 1.0 M ethanol as electrolyte, at least 10 cycles of cyclic voltammetry were carried out before regular voltammograms were recorded. Throughout the cyclic voltammetry experiments, the potential window was set between -0.2 V and 0.6 V. Prior to experiments, the electrolytes were degassed by bubbling with nitrogen for 30 min. For comparisons, consistent amounts of Au RLNPs were used for growing Au RLNP@SiO_2 NPs or for treatment with HCl. Fabrication of working electrodes using Au RLNP@SiO_2 NPs, and HCl-treated Au RLNPs was carried out as

above.

Characterization

The nanoparticles were imaged using a Hitachi S-4800 scanning electron microscope (SEM), and a JEOL JEM-2010 Luminography (Fuji FDL-5000) Ultramicrotome (CRX) transmission electron microscope (TEM). Samples were prepared for TEM by concentrating the nanoparticle mixture by centrifuging twice for 5 min at 13500 rpm with resuspension in 100 µL of nanopure water and immobilizing 10-µL portions of the solution on Formvar-coated Cu grids. Extinction spectra were recorded with a UV-Vis spectra spectrometer (UVIKON XS). Solution pH was measured using an Orion 420 A+ pH meter. Powder X-ray diffraction (PXRD) was performed with a RIGAKU Ultima IV diffractometer using Cu Kα radiation (wavelength 1.541 Å) in focused beam and a continuous scan rate of 0.09° min^{-1} in the range 30-90°. The IR spectra of Au RLNPs and Au RLNP@SiO_2 NPs in the range 399–4000 cm^{-1} were recorded using KBr pellets on a FT/IR-4200 JASCO spectrometer (JASCO FT/IR-4200 spectrometer).

Results and Discussion

Initially, the highly monodisperse Au RLNPs (the average diameter was 66.5 ± 16.1 nm, Fig. 1a and Fig. S1a) were prepared according to protocols developed previously.[20] The PXRD pattern of Au RLNPs reveals that the Au RLNPs are composed of pure crystalline gold (Fig. S1b, all peaks can be indexed to reflections of the face-centered cubic (fcc) structure of metallic gold, (*Au,* JCPDS card No. 03-065-2870)). PVP, an amphiphilic and nonionic polymer, is generally used as a stabilizing agent in the synthesis of colloidal nanoparticles.[27] It has also been applied to increase the interaction between silica and gold during preparation of Au core – SiO_2 shell nanoparticles.[28,29] Herein, PVP was employed to protect the high-energy surface of Au RLNPs and as a primer for the direct growth of silica to form Au RLNP@SiO_2 NPs. The scanning electron microscopy (SEM) and transmission electron microscopy (TEM) images of Au RLNP@SiO_2 NPs (Fig. 1b-d and Fig. S2) show the well-established core-shell structure in which the as-synthesized Au RLNPs were uniformly and individually encompassed within silica shells while still sustaining their rough and edge-rich surfaces. No Au RLNPs were observed without silica coating, and this demonstrates that the synthetic strategy is effective and high-yielding for the growth of SiO_2 shell on the surface of Au RLNP core. The average diameter of individual Au RLNP@SiO_2 NPs was 91.8±12.5 nm (148 particles were evaluated, Fig. 1e) with the mean size of gold cores nearly similar to that of Au RLNPs before silica-coating (Fig. S1). As shown in Fig. 1f, the SPR band of PVP-capped Au RLNPs remained almost unaltered whereas a red shift of 10 nm was observed upon silica deposition because of an increase in the local refractive index produced by the silica shells.[30,31] However, almost no differences in SPRs of Au RLNPs and Au RLNP@SiO_2 NPs except a red shift of 10 nm strongly demonstrate that the morphology of Au RLNPs was not critically changed after silica coating. The existence of strong absorption bands in the FT-IR spectrum of Au RLNP@SiO_2 NPs at 1097 cm^{-1} and 941 cm^{-1} corresponds to the asymmetric stretching vibrations of the Si−O−Si and Si−O(H) bonds from the silica layer (Figure S3).[49] These two peaks, however, are not observed in case of Au RLNPs, further confirming the successful silica encapsulation step.

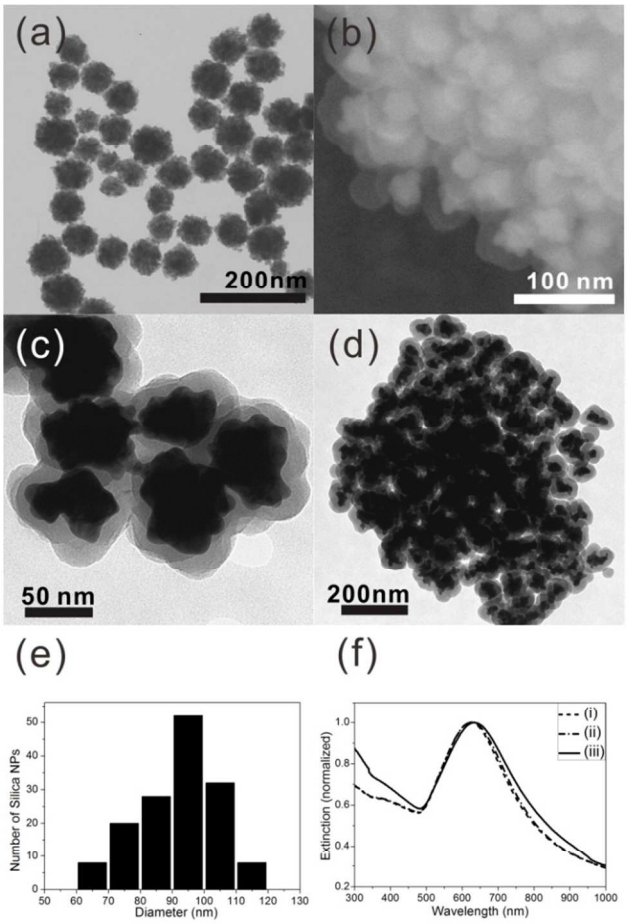

Figure 1. (a) Transmission electron microscopy (TEM) image of Au RLNPs; (b) Scanning electron microscopy (SEM) image of Au RLNPs@SiO_2NPs; (c) and (d) TEM images of Au RLNPs@SiO_2 NPs; (e) Size distribution of Au RLNPs@SiO_2 NPs; (f) UV-Vis spectra for different nanoparticle suspensions. Legend for (f): (i) Au RLNPs (dotted), (ii) Au RLNPs with PVP (PVP-capped Au RLNPs, dashed-dotted), and (iii) Au RLNPs@SiO_2 NPs (solid).

It is well recognized that the high roughness and plethora of edge-rich surfaces comprising high-index facets, could be the origin of the nanoparticles' superior catalytic performance.[16] Thus, it necessitates assessing whether the catalytically active surfaces of the synthesized nanoparticles are stable in a variety of environments. In the current study, CTAB, MPTS, and HCl were introduced into the colloidal solution of as-synthesized Au RLNPs in order to investigate the structural stability of the nanoparticles in different ambient conditions. Fig. 2 shows typical SEM images demonstrating changes in geometries of

Au RLNPs upon adding the reagents. As shown in Fig. 2a and 2b, similar agglomeration and size changes were observed upon adding either CTAB or MPTS, although the raspberry-like motifs (i.e., rough surface area) of gold nanoparticles were not significantly changed. The surface plasmon resonance (SPR) changes shown in the UV-Vis spectra further confirmed the structural changes of Au RLNPs treated with CTAB and MPTS (Fig. 2c, and Fig. S4 and S5). The introduction of such reagents might lead to aggregation of Au RLNPs.

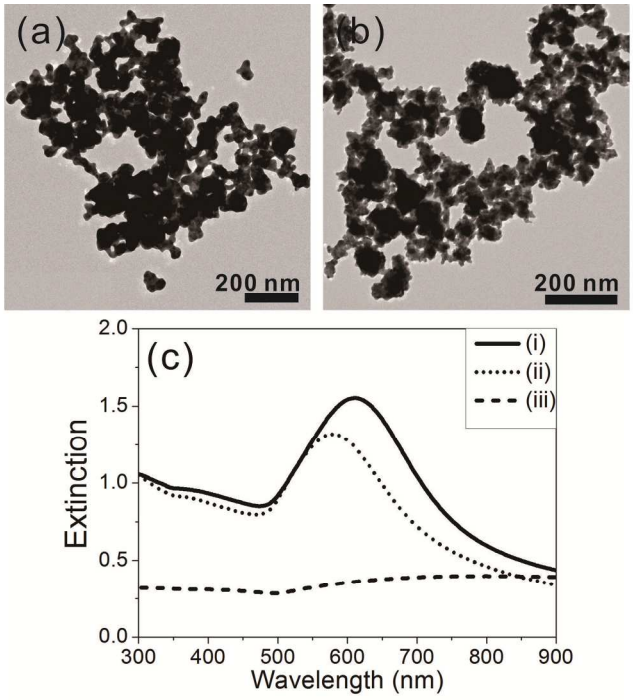

Figure 2. Morphological changes of Au RLNPs after adding: (a) CTAB (*aq*) (100 µL; 100 mM) and (b) MPTS (5 µL in EtOH (1 mL)); (c) UV-Vis spectra corresponding to the different nanoparticle suspensions (24 hour after addition). Legend for (c): (i) Au RLNPs (solid), (ii) CTAB-treated Au RLNPs (dotted), and (iii) MPTS-treated Au RLNPs (dashed).

With the HCl treatment (HCl-treated Au RLNPs), it was experimentally observed that Au RLNPs collectively collapsed into pseudo spherical nanoparticles with smooth surfaces (Fig. 3a); this corresponds to a blue-shift in the UV-Vis spectrum towards around 520 nm, recognized to the surface plasmon resonance (SPR) of gold nanospheres. This morphological change can be attributed to the oxidative etching that has been employed to control the size and shape of other noble metal nanostructures.[32-34] On the other hand, the Au RLNP@SiO_2 NPs exhibited no geometrical change when HCl was added (HCl-treated Au RLNP@SiO_2 NPs). In Fig. 3b, TEM images show that the Au RLNPs core in Au RLNP@SiO_2 NPs still retained their original raspberry-like morphology without any observable agglomeration. This observation is also consistent with results obtained from UV-Vis spectra, indicating no detectable shift in the SPR peak of the core-shell nanoparticles after HCl was added in Au RLNP@SiO_2 NPs ((ii) in Fig. 3c *vs* (ii) in Fig. 1f).

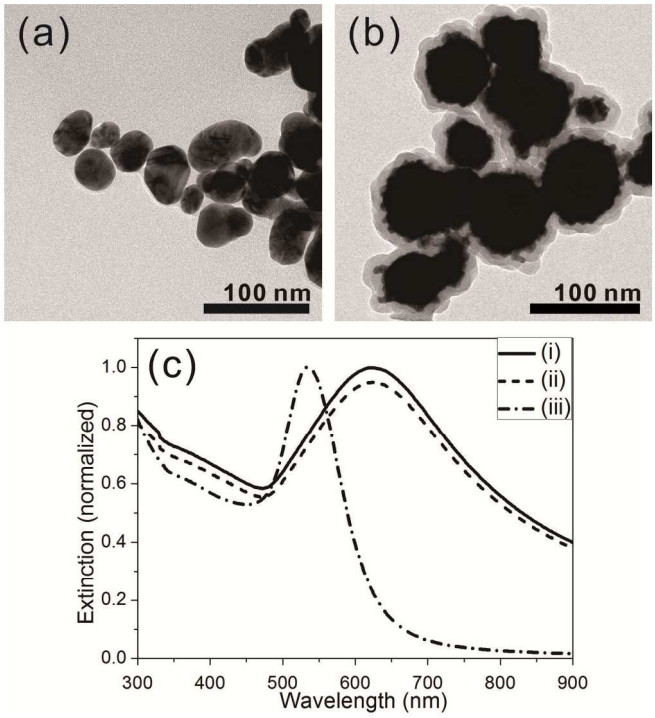

Figure 3. TEM images of (a) HCl-treated Au RLNPs and (b) HCl-treated Au RLNP@SiO_2 NPs; (c) the corresponding UV-Vis spectra of nanoparticle suspensions. Legend for (c): (i) Au RLNPs (solid), (ii) HCl-treated Au RLNP@SiO_2 NPs, and (iii) HCl-treated Au RLNPs (dashed-dotted).

Direct ethanol fuel cells (DEFC) have attracted much attention in recent years because ethanol has a higher theoretical energy density (8.01 kW·h kg^{-1}) than methanol (6.09 kW·h kg^{-1}) and formic acid (1.74 kW·h kg^{-1}), has a relative low toxicity, and also fewer environmental issues.[35,36] Another advantage is that ethanol is a renewable source that can be massively produced by the chemical industry or by fermentation of biomass.[37] In order to assess electrocatalytic activity of the synthesized Au RLNPs, ethanol electrooxidation in KOH solution was carried out. Cyclic voltammograms using electrodes modified with Au RLNPs, HCl-treated Au RLNPs, and Au RLNP@SiO_2 NPs are shown in Fig. 4. These cyclic voltammograms demonstrate similarities to other catalytic systems reported recently.[20,38-42] The HCl-treated Au RLNP-modified electrode showed an oxidation peak at about 0.23 V, which is 30 mV more positive than that of the Au RLNP-modified electrode. Moreover, the oxidation current for the HCl-treated Au RLPN-modified electrode was around 0.55 mA, much less than for the Au RLNP-modified electrode (1.54 mA). These results indicate that the Au RLNP-modified electrode has substantially higher electrocatalytic activity than the HCl-treated Au RLNP-modified electrode. The catalytic enhancement of Au RLNPs is attributed to the existence of highly energetic surfaces in raspberry-like morphologies. In contrast, Au RLNP@SiO_2 NPs do not show any electrocatalytic activities over the entire potential window. This may result from electron transfer between the gold and electrode surfaces being hindered by the insulating silica shell.[43]

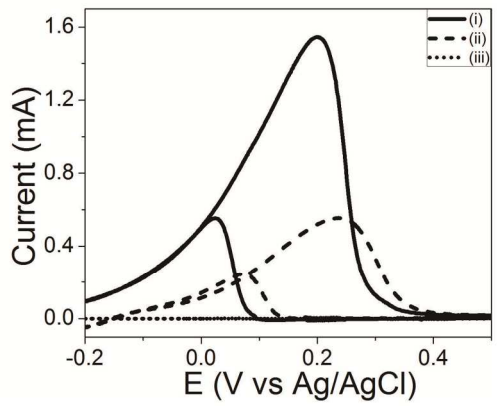

Figure 4. Cyclic voltammograms (CVs) of the catalysis of (i) Au RLNPs; (ii) HCl-treated Au RLNPs; (iii) Au RLNPs@SiO_2 NPs in ethanol electrooxidation. Each CV was measured in a solution of 1.0 M ethanol with 0.5 M KOH at 20 mV/s.

Catalytic reduction of 4-nitrophenol (4-NP) to 4-aminophenol in the presence of $NaBH_4$ was chosen as a model reaction to evaluate the catalytic performance of Au RLNPs and Au RLNP@SiO_2 NPs.[44-47] It is well established that reduction of 4-NP by $NaBH_4$ is thermodynamically feasible but kinetically restricted without a catalyst.[48] Progress of the reduction reaction was monitored by the UV-Vis absorption spectrum after addition of catalysts. The characteristic absorption peak of 4-NP aqueous solution was located at 396 nm after $NaBH_4$ had been added. Notably, in the absence of catalysts the reduction reaction of 4-NP did not proceed, even with a large excess of $NaBH_4$. However, when catalysts were introduced, the reduction of 4-NP was clearly observed. The absorption by the reaction mixture at 400 nm gradually decreased as the reaction proceeded, along with a concurrent increase of the 4-aminophenol peak at 300 nm. Fig. S6 shows

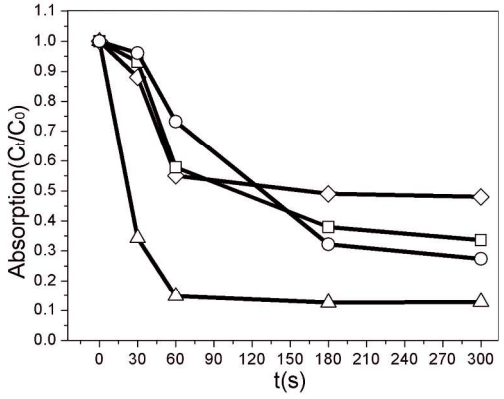

Figure 5. UV-Vis spectral changes of 4-nitrophenol (4-NP) as a function of reaction time. The relationships of absorption (C_t/C_0, absorbances at 400 nm) versus reaction time (t) in reductions catalyzed by Au RLNPs (△), HCl-treated Au RLNPs (◇), Au RLNPs@SiO_2 (□), and HCl-treated Au RLNPs@SiO_2 (○).

the UV-Vis spectra of 4-NP as a function of reaction time in the presence of Au RLNPs, HCl-treated Au RLNPs, Au RLNP@SiO_2 NPs, and HCl-treated Au RLNP@SiO_2 NPs (Fig. S6 (a) to (d), respectively). Fig. 5 shows the concentration of 4-NP plotted versus time, providing a comparison of the catalytic activities of Au RLNPs and Au RLNP@SiO_2 NPs (C_t: absorption by 4-NP at specific reaction time, t; C_0: initial absorption by 4-NP as catalysis starts). The rate constants in different systems calculated based on the slope of the linear fit of $-\ln(C_t/C_0)$ versus time (Fig S7). As can be seen, Au RLNPs exhibited higher catalytic activity than their core-shell counterparts (Au RLNP@SiO_2 NPs, and HCl-treated Au RLNP@SiO_2 NPs), possibly owning to the silica shell hindering diffusion of reactants to the inner active gold sites. Furthermore, HCl-treated Au RLNPs, suffering from much degradation of surface roughness, show much worse catalytic performance than other catalyst systems (Fig. 5).

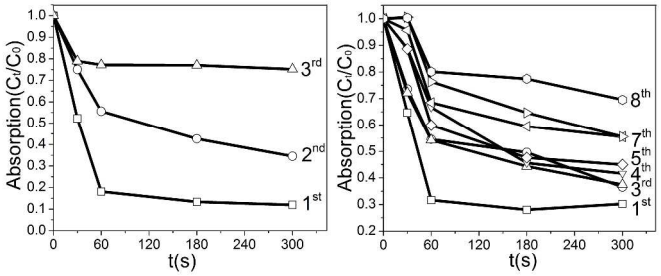

Figure 6. The 4-NP absorption ratio (C_t/C_0, at 400 nm) versus reaction time (t) over (a) Au RLNPs and (b) Au RLNPs@SiO_2 . The numbers represent repeated catalytic cycles.

We also investigated the degree of reusability of the two catalysts. As shown in Fig. 6a and Fig. S8, the conversion (conversion = $1-C_t/C_0$) of 4-NP decreases dramatically from 0.88 to 0.25 after Au RLNPs were only used 3 times while Au RLNP@SiO_2 NPs still retained good catalytic performance for up to 7 cycles. The conversion of 4-NP upon Au RLNP@SiO_2 NPs slightly decreases from around 0.70 (1^{st} cycle) to 0.45 (7^{th} cycle). These results indicate that the stability and reusability of Au RLNPs improved significantly after encapsulation into a silica shell, maintaining their catalytic activity, and enabling potential for practical applications.

Conclusions

In conclusion, raspberry-like gold nanoparticles (Au RLNPs) show high catalytic activities for 4-nitrophenol reduction and ethanol electrooxidation owing to their high surface area. The stability and applicability of Au RLNPs were significantly improved by silica encapsulation through a simple sol-gel process. Polyvinylpyrrolidone (PVP) was used as a polymeric stabilizer and a primer prior to condensation of the TEOS. The resulting Au RLNP@SiO_2 NPs showed great enhancement in stability under strongly acidic conditions.

Acknowledgements

This research was supported by Basic Science Research Program through the National Research Foundation of Korea (NRF) funded

by the Ministry of Education, Science and Technology (NRF–2013R1A1A2057675) and by Hallym University Research Fund 2012 (HRF-G-2012-3)

Notes and references

Department of Chemistry, Hallym University, Chuncheon, Gangwon-do, 200-702, Republic of Korea

Electronic Supplementary Information (ESI) available: [details of any supplementary information available should be included here]. See DOI: 10.1039/b000000x/

1 S. Linic, P. Christopher and D. B. Ingram, *Nat. Mater.*, 2011, **10**, 911-921.
2 R. Jiang, B. Li, C. Fang and J. Wang, *Adv. Mater.*, 2014, **26**, 5274-5309.
3 M. Lin, H. Pei, F. Yang, C. Fan and X. Zuo, *Adv. Mater.*, 2013, **25**, 3490-3496.
4 Y. Zhang, Y. Guo, Y. Xianyu, W. Chen, Y. Zhao and X. Jiang, *Adv. Mater.*, 2013, **25**, 3802-3819.
5 O. Tokel, F. Inci and U. Demirci, *Chem. Rev.*, 2014, **114**, 5728-5752.
6 A. T. Bell, *Science*, 2003, **299**, 1688-1691.
7 Vines, F. Gomes, J. R. B. and F. Illas, Chem. Soc. Rev. 2014, 43, 4922.
8 Y. Xiong and Y. Xia, *Adv. Mater.*, 2007, **19**, 3385-3391.
9 H. Yoo, J. Sharma, H.-C. Yeh and J. S. Martinez, *Chem. Commun.*, 2010, **46**, 6813-6815.
10 H. Yoo, J. Sharma, J. K. Kim, A. P. Shreve and J. S. Martinez, *Adv. Mater.*, 2011, **23**, 4431-4434.
11 S. Tawfick, M. D. Volder, D. Copic, S. J. Park, R. Oliver, E. S. Polsen, M. J. Roberts and A. J. Hart, *Adv. Mater.*, 2012, **24**, 1628-1674.
12 M. R. Jones, K. D. Osberg, R. J. Macfarlane, M. R. Langille and C. A. Mirkin, *Chem. Rev.*, 2011, **111**, 3736-3827.
13 T. K. Sau and A. L. Rogach, *Adv. Mater.*, 2010, **22**, 1781-1804.
14 C.-L. Lu, K. S. Prasad, H.-L. Wu, J. A. Ho and M. H. Huang, *J. Am. Chem. Soc.*, 2010, **132**, 14546-14553.
15 M. Chen, B. Wu, J. Yang and N. Zheng, *Adv. Mater.*, 2012, **24**, 862-879.
16 Z. Quan, Y. Wang and J. Fang, *Acc. Chem. Res.*, 2013, **46**, 191-202.
17 Y. Zhang, Q. Xiao, Y. Bao, Y. Zhang, S. Bottle, S. Sarina, B. Zhaorigetu and H. Zhu, *J. Phys. Chem. C*, 2014, **118**, 19062-19069.
18 X. Liu, L. He, Y.-M. Liu and Y. Cao, *Acc. Chem. Res.*, 2014, **47**, 793-804.
19 Y. Zhang, X. Cui, F. Shi and Y. Deng, *Chem. Rev.*, 2012, **112**, 2467-2505.
20 M. H. Jang, J. K. Kim and H. Yoo, *J. Nanosci. Nanotechnol.*, 2012, **12**, 4088-4092.
21 R. G. Chaudhuri and S. Paria, *Chem. Rev.*, 2012, **112**, 2373-2433.
22 N. R. Jana, C. Earhart and J. Y. Ying, *Chem. Mater.*, 2007, **19**, 5074-5082.
23 N. Erathodiyil and J. Y. Ying, *Acc. Chem. Res.*, 2011, **44**, 925-935.
24 J. Park and H. Yoo, *Microporous Mesoporous Mater.*, 2014, **185**, 107-112.
25 L. M. Liz-Marzán, M. Giersig and P. Mulvaney, *Langmuir*, 2005, **12**, 4329-4335.
26 M. Schulzendorf, C. Cavelius, P. Born, E. Murray and T. Kraus, *Langmuir*, 2011, **27**, 727-732.
27 G. Collins, M. Schmidt, G. P. McGlacken, C. O'Dwyer and J. D. Holmes, *J. Phys. Chem. C*, 2014, **118**, 6522-6530.
28 A. Guerrero-Martínez, J. Pérez-Juste and L. M. Liz-Marzán, *Adv. Mater.*, 2010, **22**, 1182-1195.
29 C. Graf, D. L. J. Vossen, A. Imhof and A. van Blaaderen, *Langmuir*, 2003, **19**, 6693-6700.
30 C. Wang, Z. Ma, T. Wang and Z. Su, *Adv. Funct. Mater.*, 2006, **16**, 1673-1678.
31 I. Pastoriza-Santos, A. Sánchez-Iglesias, F. J. García de Abajo and L. M. Liz-Márzan, *Adv. Funct. Mater.*, 2007, **17**, 1443-1450.
32 B. Li, R. Long, X. Zhong, Y. Bai, Z. Zhu, X. Zhang, M. Zhi, J. He, C. Wang, Z.-Y. Li and Y. Xiong, *Small*, 2012, **8**, 1710-1716.
33 M. Liu, Y. Zheng, L. Zhang, L. Guo and Y. Xia, *J. Am. Chem. Soc.*, 2013, **135**, 11752-11755.
34 C.-Y. Chiu, M.-Y. Yang, F.-C. Lin, J.-S. Huang and M. H. Huang, *Nanoscale*, 2014, **6**, 7656-7665.
35 W. Hong, J. Wang and E. Wang, *ACS Appl. Mater. Interfaces*, 2014, **6**, 9481-9487.
36 E. Antolini and E. R. Gonzalez, *J. Power Sources*, 2010, **195**, 3431-3450.
37 M. Balat and H. Balat, *Appl. Energ.*, 2009, **86**, 2273-2282.
38 J. Huang, X. Han, D. Wang, D. Liu and T. You, *ACS Appl. Mater. Interfaces*, 2013, **5**, 9148-9154.
39 A.-L. Wang, H. Xu, J.-X. Feng, L.-X. Ding, Y.-X. Tong and G.-R. Li, *J. Am. Chem. Soc.*, 2013, **135**, 10703-10709.
40 H. M. Song, D. H. Anjum, R. Sougrat, M. N. Hedhili and N. M. Khashab, *J. Mater. Chem.*, 2012, **22**, 25003
41 Z.-B. Wang, P.-J. Zuo, G.-J. Wang, C.-Y. Du and G.-P. Yin, *J. Phys. Chem. C*, 2008, **112**, 6582-6587.
42 K. S. Meher and G. R. Rao, *J. Phys. Chem. C*, 2013, **117**, 4888-4900.
43 Y. Kobayashi, T. Iwasaki, K. Kageyama, S. Ishikuro, K. Yamasaki, T. Yonezawa and A. Takenoshita, *Colloids Surf., A*, 2014, **457**, 244-249.
44 J. Lee, J. C. Park and H. Song, *Adv. Mater.*, 2008, **20**, 1523-1528.
45 S. Panigrahi, S. Basu, S. Praharaj, S. Pande, S. Jana, A. Pal, S. K. Ghosh and T. Pal, *J. Phys. Chem. C*, 2007, **111**, 4596-4605.
46 J. Ge, Q. Zhang, T. Zhang and Y. Yin, *Angew. Chem. Int. Ed.*, 2008, **47**, 8924-8928.
47 F.-H. Lin and R.-A. Doong, *J. Phys. Chem. C*, 2011, **115**, 6591-6598.
48 Y. Chi,; J. Tu, M. Wang, X. Li and Z. Zhao, *J. Colloid Interface Sci.*, 2014, **423**, 54-59.
49 S. Liu; M. Han, *Adv. Funct. Mater.* 2005, **15**, 961-967.

